

Enhanced electrical and optoelectrical properties of cadmium selenide nanobelts by chlorine doping

Lijie Zhang^{1,2}, Hongfei Yu², Wei Cao², Chao Zou², Youqing Dong², Da-Ming Zhu^{1,3}, Shaoming Huang²

¹Shanghai Institute of Technical Physics, Chinese Academy of Sciences, Shanghai 200083, People's Republic of China

²Nanomaterials and Chemistry Key Laboratory, Wenzhou University, Wenzhou 325027, People's Republic of China

³Department of Physics and Astronomy, University of Missouri-Kansas City, Kansas City, Missouri 64110, USA

E-mail: smhuang@wzu.edu.cn

Published in Micro & Nano Letters; Received on 27th October 2013; Revised on 19th November 2013; Accepted on 10th December 2013

Single-crystalline chlorine-doped cadmium selenide (CdSe) nanobelts (NBs) with a wurtzite structure were synthesised by using CdSe and InCl₃ powder as sources via a co-evaporation approach. The investigation of the performance of the field-effect transistors fabricated from Cl-doped NBs shows *n*-type conduction behaviour and enhanced conductivity (1–70 S/cm). Furthermore, it is found that the photoconductivity (illuminated by a white light with a power density of 1.3 mW/cm²) increases with the enhancement of the conductivity. Photoconductive analysis reveals that the Cl-doped NBs show excellent photoresponse properties, with responsivity of 8.87×10^5 AW⁻¹ and a corresponding external quantum efficiency of 1.74×10^6 when illuminated under a 650 nm light and biased 1 V. In addition, the electrical properties of the Cl-doped NBs can be influenced by changing the ambience, which is caused by their surface states.

1. Introduction: Cadmium selenide (CdSe) one-dimensional (1D) nanostructures, including nanowires (NWs) and nanobelts (NBs), are considered to be excellent building blocks for assembling nanoscale electronics and optoelectronics, such as field-effect transistors (FETs) [1–4], lasers [5], photodetectors [6–9], solar cells [10–12] and so on. However, the intrinsic CdSe nanostructures usually exhibit poor conductivity, resulting in low performances of the nanostructure-based devices. Appropriate doping is an efficient approach to tune the electrical properties of the CdSe nanostructures. Recently, CdSe NWs with tunable conductivity were realised by using indium (In) [2] or gallium (Ga) [3] as *n*-type dopant. The CdSe NBs with high conductivity were synthesised by a Cd-enriched growth method [1]. In addition, several other dopants were employed to enhance the electrical properties of the II–VI semiconductors. For example, the conductivity and photoconductivity of CdS NWs were greatly enhanced by chlorine (Cl)-doping [13]. Therefore, Cl is probably an active dopant for improving the electrical properties of the CdSe nanostructures. Most recently, Cl-doped CdSe NBs were synthesised by using CdCl₂ as the dopant and employed in the fabrication of a Schottky diode with an Au contact [14]. However, the properties of the doped NBs, for example the conductivity and photoconductivity distribution, the influence of surface states on the electron transport or optoelectrical properties and so on, are still unknown. In addition, the CdCl₂ always contains crystalline water, which makes difficulties in the synthesis process. For example, a pretreatment (200°C for 2 h in nitrogen atmosphere) is necessary to eliminate the crystalline water [14].

In this reported work, Cl-doped CdSe NBs were synthesised by a facile co-evaporation method using InCl₃ and CdSe powder as source materials. Back-gate FETs based on a single NB were fabricated and investigated. The results indicate *n*-type conduction behaviour and improved conductivity of the NBs. Experimentally, the conductivity of the NBs was in the range 1–70 S/cm. In addition to the geometric parameters of the device (e.g. NB width and distance between two electrodes) and the experimental conditions, the photoconductivity depends on the inherent nature of the NBs (e.g. conductivity). The relationship between conductivity and photoconductivity (under an illumination of a white light with a power density of 1.3 mW/cm²) demonstrates that the photoconductivity increases with increasing conductivity. The single-NB-based

photodetectors were fabricated and showed high responsivity (e.g. 8.87×10^5 AW⁻¹). As is known, the excellent optoelectronic and electrical properties of the 1D nanomaterials are mainly because of their large surface-to-volume ratio. In other words, the surface states of the 1D nanostructures play an important role in their performance for nanodevices. Generally, the electrical or optoelectrical performance of the NB-based devices varies with the ambience around the NBs. In this work, we examined the effect of the surface state on the electrical properties of the NBs through measuring the *I*–*V* characteristic at different ambiances.

2. Experimental

2.1. Synthesis of the materials: The Cl-doped CdSe NBs were synthesised via a chemical vapour deposition (CVD) process [15] in a horizontal tube furnace. A quartz boat loaded with CdSe powder (99.999%, Alfa Aesar) was placed in the centre of the furnace, another quartz boat loaded with InCl₃ powder (99.99%, Alfa Aesar) was placed at an upstream zone ~15 cm away from the CdSe source and silicon wafer with 30 nm-thick Au film was placed at a downstream zone ~11 cm away from the CdSe source to collect the products. The system was pumped down to a base pressure of ~20 Pa, and then flushed with high-purity argon for 30 min to remove residual oxygen. Then the system was elevated to a growth temperature (720°C) in 15 min. The growth continued for 30 min under a pressure of 600 Pa and flowing argon (150 sccm). During the growth process, the temperature of the InCl₃ source and the Si substrate were 300–400°C and 550–600°C, respectively. After growth, the system was naturally cooled down to room temperature. Then the products with brownish black were obtained. Undoped CdSe NBs were also synthesised under the same conditions except the use of the InCl₃ source, which was used for comparison of the electrical and optoelectrical properties with the Cl-doped NBs.

2.2. Characterisation: The products were characterised by field emission scanning electron microscopy (SEM, FEI NanoSEM 200) with a energy dispersive X-ray spectrometer (EDS, EDAX Inc.), transmission electron microscopy (TEM, JEOL 2100F), X-ray powder diffraction (XRD, Bruker D8 advanced X-ray diffractometer using CuK α radiation: $\lambda = 0.15418$ nm) and X-ray photoelectron spectroscopy (XPS, Kratos AXIS Ultra DLD).

2.3. Device fabrication and measurements: Back-gate FETs and photodetectors were fabricated by dispersing the NBs on SiO₂ (300 nm)/Si substrates and subsequently using electron beam lithography or copper-grid mask-based lithography to define electrodes, followed by metallisation using thermal evaporation (200 nm indium and 50 nm gold) and lift off.

The current–voltage (I – V) characteristics and time response of the devices were recorded in air or in a SEM chamber (limiting vacuum: $\sim 3 \times 10^{-4}$ Pa) and at room temperature by a semiconductor characterisation system (4200 SCS, Keithley Instruments Inc., USA). A xenon lamp (500 W) combined with a monochromator (Zolix Instruments Co. Ltd, China) and a 532 nm laser were employed to supply the monochromatic light. The photoconductivity was evaluated by measuring the I – V curves of devices under the illumination of an incandescent lamp (1.3 mW/cm²). The light intensities were calibrated by a standard silicon photodetector.

3. Results and discussion

3.1. Morphologies, composition and structures of the as-synthesised Cl-doped CdSe NBs: The SEM observation indicates that as-synthesised NBs are several hundreds of micrometres to millimetres in length and they uniformly cover the whole surface of Si substrates (Fig. 1a) and the NBs have a clean and smooth surface (Fig. 1b). The NBs are usually sub-micrometre to micrometres in width and 20–150 nm in thickness. The inset in Fig. 1b shows an enlarged SEM image of a single NB with a thickness of 38 nm. A low-magnification TEM image (Fig. 1c) further confirms the belt-like geometry of the products. The interplanar d -spacings of 0.36 and 0.69 nm in a high-resolution TEM image (Fig. 1d) correspond to the (100) and (001) lattice planes of CdSe, respectively. A selected area electron diffraction (SAED) pattern (Fig. 1e) reveals the single-crystal hexagonal structure of the NBs. A typical XRD pattern of the NBs is given in Fig. 1f. Except a Si signal from the substrates, all other peaks are in agreement with bulk wurtzite CdSe (JCPDS 08-0459). No impurity peaks in the XRD pattern indicates that the CdSe NB structure has not been changed because of the Cl doping. Strong Cd, Se peaks and a weak Cl peak are observed in the EDS results (Fig. 1g) measured using a 15 keV electron beam in the SEM, but no signals from In can be found in the EDS spectrum. Fig. 1h shows a typical XPS spectrum of the NBs. In addition to the strong Cd and Se signals, a weak peak at ~ 198 eV corresponding to the Cl 2p_{3/2} core-level emission was observed. Similar to the EDS results, no signals of In can be detected by XPS. The EDS and XPS results indicate the successful Cl doping in the CdSe NBs. While no In signals exist in both the EDS and XPS results, it cannot exclude the possibility that In was doped in the CdSe NBs. According to the previous investigations [2], the In-doped CdSe NWs can be synthesised via the co-evaporation method using metal In and CdSe powder as sources. Here, the impurities originate from the composite precursor of InCl₃. Thus, the amount of In may be much smaller than that of Cl in the NBs, leading to detection not being possible. Note that the undoped CdSe NBs synthesised at the same conditions except the use of InCl₃ source show a similar morphology and crystal structure.

3.2. FETs based on single Cl-doped CdSe NB: To determine the effect of Cl doping on the electrical transport properties of the CdSe NBs, the FETs based on a single Cl-doped NB were fabricated and investigated. Fig. 2a shows a typical source-drain current (I_{ds}) against source-drain voltage (V_{ds}) curves of a back-gate FET when the gate-source voltage (V_{gs}) is swept from -10 to 10 V. The inset gives a schematic illustration of the FET. The linearity of the I_{ds} – V_{ds} characteristics indicates good ohmic contacts between the NB and metal electrodes. The electrical conductance enhances with the enhancement of V_{gs} , indicating the n -type conduction behaviour of the FET. A typical I_{ds} – V_{gs} characteristic of the FET at a V_{ds} of 1 V is plotted in Fig. 2b. No

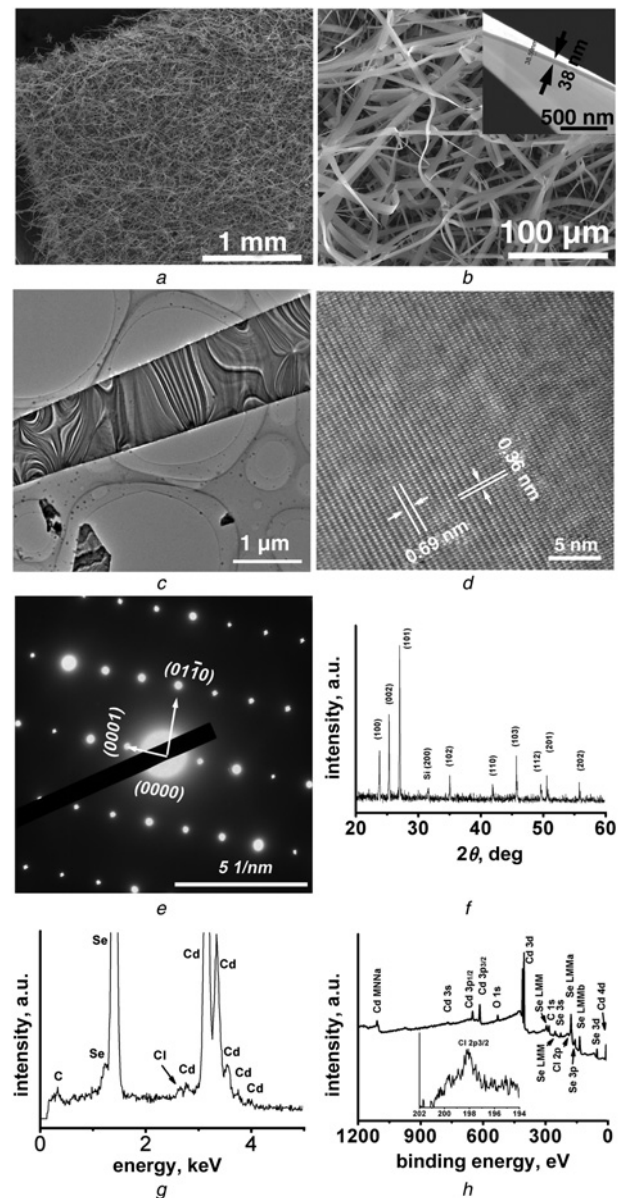


Figure 1 Low magnification SEM image of Cl-doped CdSe NBs (Fig. 1a); high-magnification SEM image of doped NBs (Fig. 1b); inset is SEM image of side of doped NBs; low resolution TEM image of NB (Fig. 1c); representative HRTEM of NBs (Fig. 1d); typical SAED pattern of NBs (Fig. 1e); XRD pattern of as-grown NBs (Fig. 1f); EDS result of NBs (Fig. 1g); XPS spectrum of NBs (Fig. 1h), inset is enlarged view of peak of Cl 2p_{3/2}

depletion arises in the range of V_{gs} from -10 to 10 V and its I_{on}/I_{off} ratio is close to 1.8. The peak transconductance (g_m) defined as dI_{ds}/dV_{gs} , which can be deduced from the slope of the I_{ds} – V_{gs} curve at $V_{ds} = 1$ V and at $V_{gs} = -10$ V, is ~ 491 nS. However, it is impossible and insignificant to evaluate the threshold voltage (V_{th}) for this FET. The capacitance of the gate dielectrics is ~ 10.9 fF obtained from the equation $C = \epsilon\epsilon_0 Lw/h$ [1], where ϵ , ϵ_0 , L , w and h represent the relative dielectric constant of SiO₂, vacuum permittivity, channel length, channel width and the thickness of SiO₂ layer. In addition, the field effect mobility, μ_e , is ~ 747.46 cm²/(Vs) at $V_{ds} = 1$ V, calculated by the equation $\mu_e = g_m L^2 / (CV_{ds})$ [2, 3]. It is difficult to directly observe the defects (e.g. vacancies or interstitial atoms) in the Cl-doped CdSe NBs by using the high-resolution TEM. Therefore, the model (vacancy or interstitial model) of Cl in the CdSe is not clear and definite. In this Letter, both the increase of Se vacancy due to the doping of Cl and the

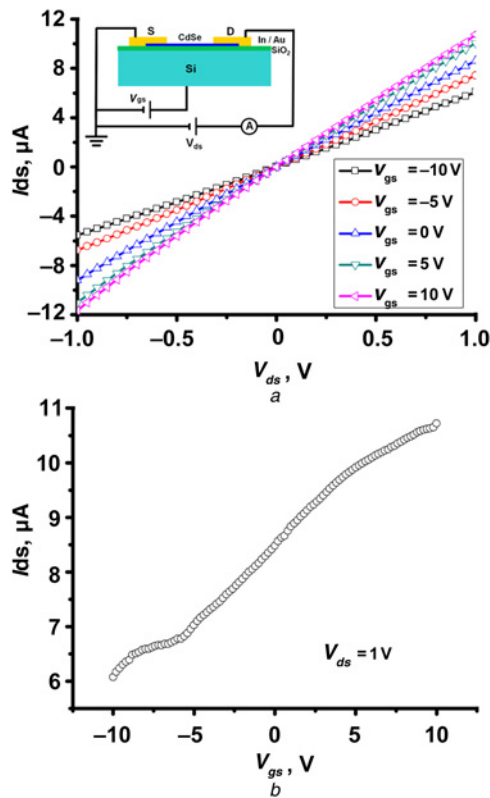


Figure 2 I_{ds} - V_{ds} curve of FET under V_{gs} changing from -10 to 10 V (Fig. 2a), inset is schematic illustration of FET; I_{ds} - V_{gs} curve at V_{ds} of 1 V (Fig. 2b)

replacement of Se^{2-} by Cl^- are possible and can result in an increase of the number of free electrons in the NBs.

3.3. Conductivity and photoconductivity of the Cl-doped CdSe NBs: It is well known that a small amount of element doping is already high enough to make a dramatic change of the electrical transport properties for a semiconductor [2, 3, 13]. To figure out the conductivity and photoconductivity of the Cl-doped NBs, two-terminal devices were fabricated by using copper grids ($30\ \mu\text{m}$ bar, $130\ \mu\text{m}$ spacing) as the mask to define electrodes. The devices based on the undoped NBs were also fabricated and investigated for comparison. Fig. 3a gives a schematic illustration of the photoconductive devices. The distances between two electrodes of the devices are in the range 20 – $25\ \mu\text{m}$. Fig. 3b shows I - V curves of an undoped NB-based device under white light ($1.3\ \text{mW}/\text{cm}^2$) illumination or in dark condition, and the dark signal has been magnified by 1000. It is difficult to fabricate good ohmic contacts between the undoped NBs and metal electrodes due to their high resistivity. Therefore, a weak current (lower than $10\ \text{pA}$ at $1\ \text{V}$) and even no signal have been obtained frequently in the dark condition for the undoped-NB-based devices. In contrast, the Cl-doped NBs exhibit much lower resistance under both dark condition and illumination of the white light, as shown in Fig. 3c. The small ratio of on/off current ($I_{\text{light}}/I_{\text{dark}}$) is probably caused by the long distance between the electrodes and high dark current due to the Cl-doping. The conductivity distribution of the Cl-doped NBs obtained by measuring more than 20 devices is in the range of 1 – $70\ \text{S}/\text{cm}$ which is approximately 5 – 7 orders of magnitude larger than that of the undoped CdSe NWs [3]. This indicates the possibility that Cl has been doped in the NBs. The photoconductivity (I_{ph}) defined by $\Delta I/(VWH)$, where ΔI is the difference between photo-excited current and dark current at a bias of V , and L , W , H are the distance between electrodes, the width of the NBs, and the thickness of the NBs, respectively, is an

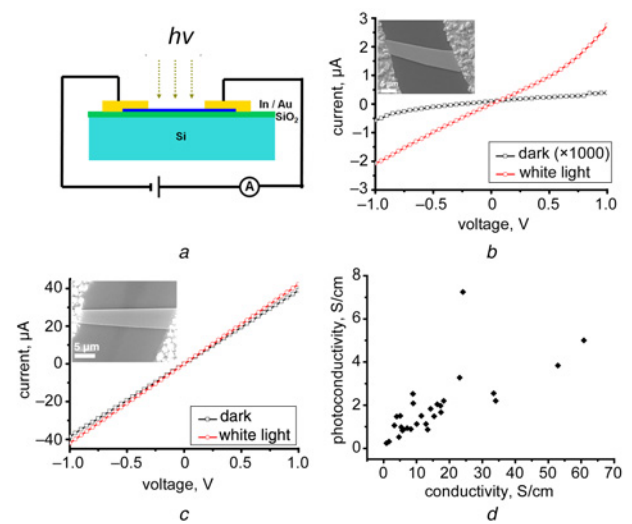


Figure 3 Schematic illustration of photoconductive devices (Fig. 3a); I - V characteristics of undoped NB-based device under illumination of white light ($1.3\ \text{mW}/\text{cm}^2$) or in dark condition (Fig. 3b), dark signal magnified by 1000; typical I - V curves of Cl-doped NB-based devices under illumination of white light ($1.3\ \text{mW}/\text{cm}^2$) or in dark condition (Fig. 3c), insets in corresponding SEM images of devices; relationship between conductivity and photoconductivity (illuminated under white light) of Cl-doped NBs (Fig. 3d)

important parameter to evaluate the photoresponse properties of NBs. The photoconductivity of the NBs depends on the geometric parameters of the device (e.g. NB width and distance between two electrodes), the experimental conditions (e.g. the bias voltage, wavelength and power density of the light) and the inherent nature of the NBs (e.g. conductivity). In this case, we assume that the geometric parameters and experimental condition are the same for all devices, that is, the photoconductivity only depends on the inherent nature. Generally, high conductivity can reduce the contact resistance between NBs and metal electrodes, resulting in that the photo-carriers pass through the contacts more easily. Therefore, it is found that the photoconductivity improves by enhancing the conductivity, as shown in Fig. 3d.

3.4. Optoelectrical properties of the Cl-doped CdSe NBs: To further evaluate the optoelectrical properties of the as-synthesised Cl-doped NBs, two terminal devices with the electrode distance of 2 – $3\ \mu\text{m}$ were fabricated and investigated. Fig. 4a shows typical I - V curves of a device under $650\ \text{nm}$ light ($1\ \text{mW}/\text{cm}^2$) illumination or under dark condition, and the inset is a SEM image of the device. The linearity of the curves indicates good ohmic contacts between the Cl-doped NB and In pads. It is found that the current increases significantly under illumination by the incident light, indicating that the NB has excellent photoresponse properties. There are two critical parameters for a photoconductive device, that is, the spectral responsivity (R_λ) and the external quantum efficiency (EQE). The former defined as the photocurrent created by the unit power of the incident light on an effective exposed area, is expressed by $R_\lambda = I_{\text{ph}}/(P_\lambda S)$, where P_λ is the light power density, and S represents the irradiated area of the NB. The latter can be deduced by the equation $\text{EQE} = hcR_\lambda/(q\lambda)$, where λ is the wavelength of the incident light, h is the Planck's constant, c is the velocity of light in vacuum and q is the electronic charge [16]. Here, the R_λ is obtained to be $8.87 \times 10^5\ \text{AW}^{-1}$, and the corresponding EQE is $1.14 \times 10^6\%$ at the voltage of $1\ \text{V}$. The $I_{\text{light}}/I_{\text{dark}}$ ratio is close to 2.

The investigation of the time response (Fig. 4b) indicates that the device is stable and reproducible. It was measured by periodically turning on and off a $650\ \text{nm}$ light ($1\ \text{mW}/\text{cm}^2$) at a voltage of $1\ \text{V}$. The photocurrent increases to 90% of its peak value in

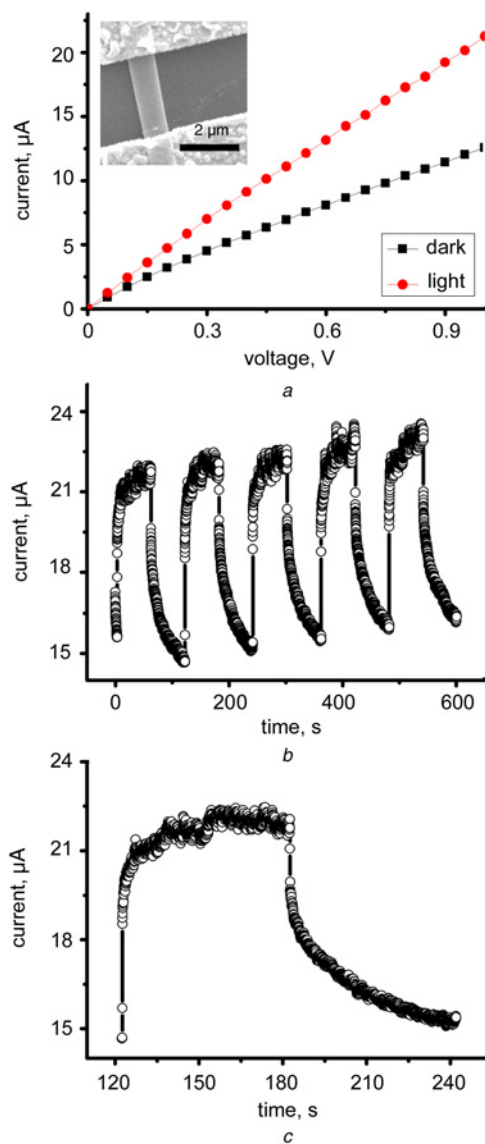


Figure 4 *I-V* curves of Cl-doped NB-based device under 650 nm-light (1 mW/cm^2) illumination or in dark condition (Fig. 4a), inset is SEM image of device; time response property of device (Fig. 4b); enlarged view of one-cycle time response (Fig. 4c)

4–5 s, and it decreases from the peak value down to $\sim 30\%$ of its peak value in 60 s. The photo-carrier lifetime of the NBs is higher than bulk due to the formation of deep level surface states in the NBs [17], which probably prolong the delay time. Generally, for a photoconductive device based on a single CdSe NB, there is a trade-off among the parameters including R_d , the $I_{\text{light}}/I_{\text{dark}}$ ratio and the photoresponse time. In other words, the device has a high R_d in that it always possesses a low $I_{\text{light}}/I_{\text{dark}}$ ratio and a long photoresponse time as well. Compared with the undoped-NB-based photoconductive device, the devices in our work exhibit much larger photocurrent but longer response time.

3.5. Effect of surface states on the electrical transport in the Cl-doped CdSe NBs: The electron transport in the Cl-doped NB can be influenced by ambiances. The *I-V* characteristics of the device measured at different ambiances (55% RH humid air, dry air or in vacuum $3 \times 10^{-4} \text{ Pa}$) at room temperature, as shown in Fig. 5a, indicates that the NB conductance can be improved in the vacuum environment. To eliminate the effect from the photo-excited carriers, the device was kept in the vacuum

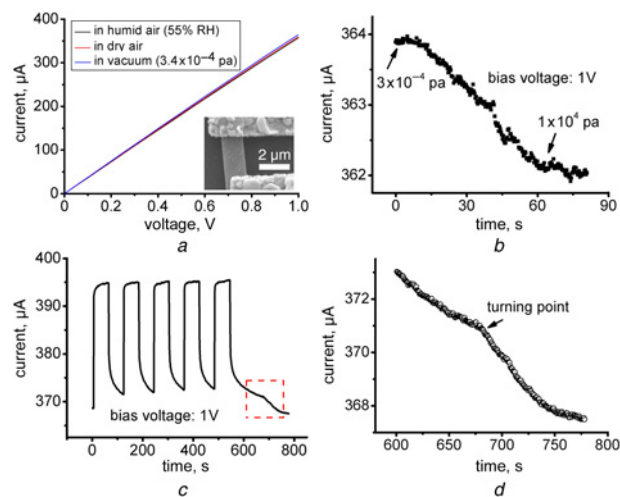


Figure 5 *I-V* characteristics of single Cl-doped NB-based device in different ambience (Fig. 5a), inset is SEM image of device; relationship between current at voltage of 1 V and pressure (Fig. 5b); time response curve of device to 532 nm-laser (1.6 mW/cm^2) at voltage of 1 V (Fig. 5c); enlarged view of curve marked by dish square in Fig. 5c (Fig. 5d)

chamber ($3 \times 10^{-4} \text{ Pa}$ in dark) for 5 h. Then the vacuum pump was turned off, followed by filling with nitrogen (N_2). The current varies with the pressure at voltage of 1 V, as shown in Fig. 5b. The current exhibits a continuous decrease with the pressure increase. The sensitivity of the current to the ambience indicates that the Cl-doped NBs can probably be employed as gas sensors. Fig. 5c shows a time response of the device that is measured by periodically turning on and off a 532 nm laser (1.6 mW/cm^2) at a bias voltage of 1 V. The device is highly stable and reproducible in vacuum ($1.8 \times 10^{-3} \text{ Pa}$). However, a turning point is found in the time response curve when the vacuum environment is changed by filling with air, as shown in the marked dish square in Figs. 5c and d (enlarged view). The effect of ambience (or pressure) on the electron transport and the recombination of photo-excited carriers is caused by the surface state of the NBs. As we know that the Cl-doped NBs have many defects in the surface, the defects act as adsorption sites and adsorb O_2 and H_2O , that is, $\text{O}_2 + e^- \rightarrow \text{O}_2^-$ and $2\text{H}_2\text{O} + \text{O}_2 + 4e^- \rightarrow 4\text{OH}^-$, and consequently, a low-conductivity depletion layer is formed near the surface [18]. Therefore the current (at a bias voltage of 1 V) decreases while pressure increases (Fig. 5b). In vacuum, the recombination of photo-excited electrons and holes mainly occurs in the NB. In air, holes migrate to the surface and discharge the negatively charged ions (O_2^- or OH^-), that is, $h^+ + \text{O}_2^- \rightarrow \text{O}_2$ or $4h^+ + 4\text{OH}^- \rightarrow 2\text{H}_2\text{O} + \text{O}_2$, and thus the recombination is accelerated (as shown in Fig. 5d).

4. Conclusion: In summary, *n*-type Cl-doped NBs with a wurtzite structure were grown via a co-evaporation method by using InCl_3 and CdSe powders as source materials. The EDS and XPS results confirm the successful doping of Cl in the CdSe NBs. As a result of the Cl-doping, the conductivity of NBs were enormously improved to be in the range 1–70 S/cm, which is approximately 5–7 orders of magnitude larger than that of the intrinsic CdSe. Furthermore, the photoconductivity (illuminated by a white light with a power density of 1.3 mW/cm^2) of the Cl-doped NBs improves with the enhancement of the conductivity. The Cl-doped NBs also exhibit excellent photoresponse properties, with a responsivity of $8.87 \times 10^5 \text{ AW}^{-1}$ and a corresponding external quantum efficiency of 1.14×10^6 when illuminated under a 650 nm-light and biased 1 V. In addition, the Cl-doped NBs show an increase of conductance and a low recombination rate of photo-carriers in vacuum instead of air, confirming that the

surface states have an effect on the electrical transport and optoelectrical properties of the Cl-doped NBs.

5. Acknowledgments: This work was supported by the NSFC (61001005, 51025207, 51102186), the NSFZJ (Y1110734), and the ZJ Key Innovative Team (2010R50014).

6 References

- [1] Liu C., Wu P., Sun T., *ET AL.*: 'Synthesis of high quality *n*-type CdSe nanobelts and their applications in nanodevices', *J. Phys. Chem. C*, 2009, **113**, pp. 14478–14481
- [2] He Z., Jie J., Zhang W., *ET AL.*: 'Tuning electrical and photoelectrical properties of CdSe nanowires via indium doping', *Small*, 2009, **5**, pp. 345–350
- [3] Hu Z., Zhang X., Xie C., *ET AL.*: 'Doping dependent crystal structures and optoelectronic properties of *n*-type CdSe: Ga nanowires', *Nanoscale*, 2011, **3**, pp. 4798–4783
- [4] Niasari S.M., Zare M.E., Sobhani A.: 'Synthesis and characterization of cadmium selenide nanostructures by simple sonochemical method', *Micro Nano Lett.*, 2012, **7**, pp. 831–834
- [5] Huang Y., Duan X., Lieber C.M.: 'Nanowires for integrated multi-color nanophotonics', *Small*, 2005, **1**, pp. 142–147
- [6] Jiang Y., Zhang W., Jie J., *ET AL.*: 'Photoresponse properties of CdSe single-nanoribbon photodetectors', *Adv. Funct. Mater.*, 2007, **17**, pp. 1795–1800
- [7] Zhao L., Hu L., Fang X.: 'Growth and device application of CdSe nanostructures', *Adv. Funct. Mater.*, 2012, **22**, pp. 1551–1566
- [8] Dai Y., Yu B., Ye Y., *ET AL.*: 'High-performance CdSe nanobelt based MESFETs and their application in photodetection', *J. Mater. Chem.*, 2012, **22**, pp. 18442–18446
- [9] Wu P., Dai Y., Sun T., *ET AL.*: 'Impurity-dependent photoresponse properties in single CdSe nanobelt photodetectors', *ACS Appl. Mater. Interfaces*, 2011, **3**, pp. 1859–1864
- [10] Yu Y., Kamat P.V., Kuno M.: 'A CdSe nanowire/quantum dot hybrid architecture for improving solar cell performance', *Adv. Funct. Mater.*, 2010, **20**, pp. 1464–1472
- [11] Zhang L., Jia Y., Wang S., *ET AL.*: 'Carbon nanotube and CdSe nanobelt Schottky junction solar cells', *Nano Lett.*, 2010, **10**, pp. 3583–3589
- [12] Dong L., Niu S., Pan C., *ET AL.*: 'Piezo-phototronic effect of CdSe nanowires', *Adv. Mater.*, 2012, **24**, pp. 5470–5475
- [13] Wu C., Jie J., Wang L., *ET AL.*: 'Chlorine-doped *n*-type CdS nanowires with enhanced photoconductivity', *Nanotechnology*, 2010, **21**, p. 505203
- [14] Du L., Lei Y.: 'Synthesis of high-quality Cl-doped CdSe nanobelts and their application in nanodevices', *Mater. Lett.*, 2013, **106**, pp. 100–103
- [15] Zhang Q., Qi J., Huang Y., *ET AL.*: 'Electron irradiation effect on the Schottky gate of ZnO nanowires-based field effect transistors', *Micro Nano Lett.*, 2011, **6**, pp. 437–440
- [16] Li L., Wu P., Fang X., *ET AL.*: 'Single-crystalline CdS nanobelts for excellent field-emitters and ultrahigh quantum-efficiency photodetectors', *Adv. Mater.*, 2010, **22**, pp. 3161–3165
- [17] Jie J., Zhang W., Jiang Y., *ET AL.*: 'Photoconductive characteristics of single-crystal CdS nanoribbons', *Nano Lett.*, 2006, **6**, pp. 1887–1892
- [18] Liao Z., Liu K., Zhang J., *ET AL.*: 'Effect of surface states on electron transport in individual ZnO nanowires', *Phys. Lett. A*, 2007, **367**, pp. 207–210